JOURNAL OF AIRCRAFT
Vol. 45, No. 6, November–December 2008

Experimental Investigation of Gurney Flaps

Mark D. Maughmer* and Götz Bramesfeld†
Pennsylvania State University, University Park, Pennsylvania 16802

DOI: 10.2514/1.37050

The aerodynamics of a Gurney-flap-equipped airfoil has been explored by means of low-speed wind-tunnel experiments performed at a chord Reynolds number of 1.0×10^6. Various chordwise locations and sizes of Gurney flaps were tested. Surface-pressure distributions and the wake momentum deficit were measured and used to determine lift, pitching moment, and drag. Compared with the clean airfoil, the measured maximum lift coefficient can be increased by nearly 30% with these simple devices. The amount of lift increase has a nearly linear dependency on the chordwise location and size of the Gurney flap. Minimum drag is primarily affected by the flap size and, to a lesser extent, by the chordwise location. The Gurney flap increases in maximum lift are obtained by increasing the lower-surface pressures over the aft part of the airfoil. At the same time, the magnitude of pressure peak on the upper surface near the leading edge is reduced such that the upper-surface pressures over the middle parts of the airfoil are reduced and the separation point is moved aft by the reduced pressure-recovery gradients. As expected, this increases the aft loading and results in an increased nose-down pitching moment. As the angle of attack is decreased, the influence of a Gurney flap extending from the lower surface likewise decreases as the flap is increasingly immersed in the thickening boundary layer. A Gurney flap mounted to the upper surface behaves in the opposite way: increasing the negative lift at low angles of attack and having less and less influence as the angle of attack is increased. Although Gurney flaps result in significantly higher drags for airfoils with extensive runs of laminar flow, this disadvantage disappears as the amount of turbulent boundary-layer flow increases, as is the case with fixed transition near the leading edge of the airfoil.

Nomenclature

C_P	=	pressure coefficient, $(p_l - p_\infty)/q_\infty$
c	=	airfoil chord
c_d	=	profile-drag coefficient
c_l	=	section lift coefficient
c_m	=	section pitching-moment coefficient about the quarter-chord point
p	=	pressure
q	=	dynamic pressure
R	=	Reynolds number based on freestream conditions and airfoil chord
x	=	airfoil abscissa
y	=	airfoil ordinate
α	=	angle of attack relative to x axis, deg

Subscripts

l	=	local point on the airfoil
max	=	maximum
∞	=	freestream conditions

Introduction

THE Gurney flap was conceived over three decades ago by race car campaigner Dan Gurney as a lift enhancement device used to increase the downforce provided by the wing of his Indianapolis 500 car. These small flaps, which are typically less than $0.02c$ in height and extend perpendicularly from the lower surface of an airfoil near its trailing edge, produce incremental increases in lift coefficient of nearly 30% [1]. Gurney flaps offer the prospect of increased values of lift in situations in which the accompanying increase in drag is not a significant detractor. In addition to the download wings of race cars, applications that have been considered include the main rotor and tail surfaces of rotorcraft, wind-turbine blades, and the main wings of heavy-lift uninhabited air vehicles [2–4].

Miniature trailing-edge effectors (MiTEs) are deployable Gurney flaps that are positioned at or near the trailing edge of a wing or rotor blade and can be deployed when needed [5]. They are typically segmented into small spanwise elements that can be individually activated. Currently, MiTEs are being explored for the simultaneous lift, pitch, roll, and yaw control of tailless fixed-wing aircraft, including the Boeing blended-wing–body concept [5], for flutter suppression [6], for enhanced rotorcraft performance [7], and for load alleviation on wind-turbine blades [8].

The goal of the research effort discussed herein is to develop relationships between the size and the location of a Gurney flap and its aerodynamic effects. Steady two-dimensional wind-tunnel measurements over a range of flap heights and chordwise locations have been made. The significance of the experimental results presented here lies in the high quality of the force and moment data, obtained using pressure integration, for an airfoil equipped with Gurney flaps, as well as the availability of surface-pressure distributions and wake surveys. Further, these measurements are the first to quantify the drag penalty due to Gurney flaps on an airfoil designed for extensive runs of laminar flow, as well as the effect on the aerodynamic characteristics when transition is fixed near the leading edge. Finally, along with being useful for the sizing of Gurney flaps for many applications, these results should be of value in validating computational fluid dynamic (CFD) predictions.

Two-Dimensional Wind-Tunnel Tests

To obtain a better understanding of Gurney flap aerodynamics, an airfoil was wind-tunnel-tested with and without Gurney flaps attached at and near the trailing edge. Lift and moment data were obtained using surface-pressure integration, whereas drag was measured using a wake-traversing probe. In addition to the baseline airfoil, configurations with Gurney flaps having heights of 0.005,

Received 11 February 2008; revision received 19 May 2008; accepted for publication 19 May 2008.

*Professor, Department of Aerospace Engineering. Associate Fellow AIAA.

†Visiting Assistant Professor, Department of Aerospace Engineering; currently Assistant Professor, Department of Aerospace and Mechanical Engineering, Saint Louis University, St. Louis, MO. Member AIAA.

0.01, and 0.02c and positioned at 0.90, 0.95, and 1.0c were tested. Data were obtained with natural and fixed transitions. Measurements were taken at a chord Reynolds number of 1.0×10^6 and Mach number of less than 0.2. Unlike most previous investigations that measured forces using a balance, the use of surface-pressure integration allows a great deal of insight as to how Gurney flaps alter the flowfield to achieve higher maximum lift coefficients.

Wind Tunnel, Model, and Data-Acquisition System

The Pennsylvania State University low-speed low-turbulence wind tunnel is a closed-throat single-return atmospheric facility. The test section is rectangular, 3.3 ft high × 4.8 ft wide, with filleted corners. The maximum test-section speed is 220 ft/s. Airfoil models are mounted vertically in the test section and attached to computer-controlled turntables that allow the angle of attack to be set. The turntables are flush with the floor and ceiling and rotate with the model. The axis of rotation corresponds to the quarter-chord of the model. The gaps between the model and the turntables are sealed to prevent leaks.

The flow quality of the Pennsylvania State University wind tunnel has been measured and documented [9]. At a velocity of 150 ft/s, the flow angularity is below ±0.25 deg throughout the test section. At this velocity, the mean velocity variation in the test section is below ±0.2%, and the turbulence intensity is less than 0.045%.

Although the attainment of high flow quality is certainly a requisite for measuring meaningful airfoil aerodynamic characteristics, additional confidence in the measurements made at Pennsylvania State University is gained by making comparisons with those taken elsewhere. For this purpose, perhaps the two most highly regarded two-dimensional low-speed wind tunnels are the Low-Turbulence Pressure Tunnel (LTPT) at the NASA Langley Research Center [10] and the Low-Speed Wind Tunnel at Delft University of Technology in The Netherlands [11]. For low-Reynolds-number airfoil aerodynamics, a benchmark set of data is that obtained with the Eppler 387 airfoil in the LTPT [12]. In Fig. 1, results from these data for $R = 2.0 \times 10^5$ to 4.6×10^5 are compared with those from the Pennsylvania State University tunnel [13]. Except for poststall aerodynamics, which are highly three-dimensional and not all that meaningful with respect to two-dimensional measurements, the agreement of the data from the two facilities is excellent. Additional comparisons of these two sets of data at Reynolds numbers down to $R = 0.6 \times 10^5$, not included here for clarity, demonstrate similar agreement [13]. In Fig. 2, Pennsylvania State University tunnel measurements made on the laminar-flow S805 wind-turbine airfoil [14] are compared with those obtained using the same wind-tunnel model at Delft University of Technology [15]. These data, at Reynolds numbers from $R = 0.7 \times 10^6$ to 1.5×10^6, also demonstrate excellent agreement. In addition to the force and moment data comparisons presented here, pressure distributions and measured transition locations also show agreement that is in accordance with those shown in [13,14].

The model used for the Gurney flap measurements is that of the 12%-thick S903 airfoil shown in Fig. 3. This airfoil was designed for use in a study exploring the effect of thickness ratio and surface roughness on the maximum lift coefficients generated by wind-turbine airfoils [16]. As an airfoil intended for wind-turbine applications, the S903 airfoil is designed to take advantage of significant runs of laminar flow; however, other than that, its thickness ratio, pitching moment, and operating range are similar to those of airfoils currently used on rotorcraft.

The 1.5 ft chord model was mounted vertically in the wind tunnel and completely spanned the 3.3 ft height of the test section. It is constructed with fiberglass skins formed in molds that were produced using a numerically controlled milling machine. The model has 33 pressure orifices on the upper surface and 32 on the lower. Each orifice has a diameter of 0.020 in. and is drilled perpendicular to the surface. The orifice locations are staggered in the spanwise direction to minimize the influence of an orifice on those downstream. The measured coordinates of the airfoil as tested, as well as the locations of the pressure orifices, are contained in [16].

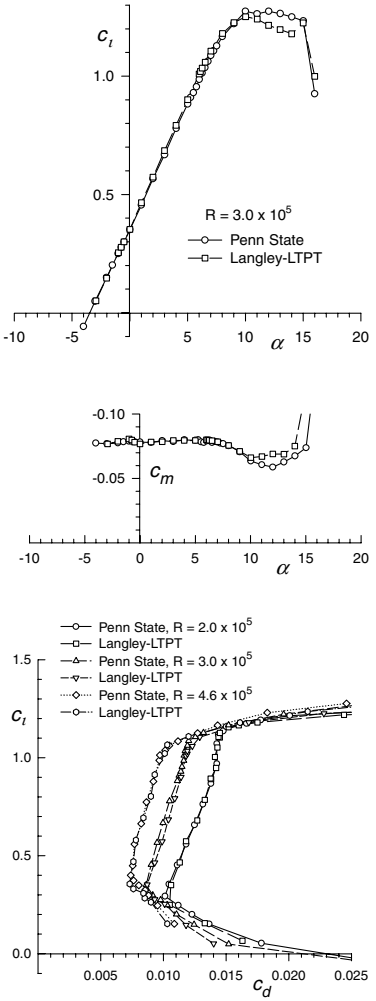

Fig. 1 Comparison of aerodynamic characteristics of the Eppler 387 airfoil measured in the low-speed wind tunnels at Pennsylvania State University and NASA Langley.

To obtain drag measurements, a wake-traversing, pitot-static pressure probe is mounted from the ceiling of the tunnel. A traversing mechanism incrementally positions the probe across the wake, which automatically aligns with the local wake streamline as the angle of attack changes. For these tests, the probe was positioned vertically at the tunnel centerline, with the nose of the probe located 0.7 chords downstream of the model trailing edge.

The basic wind-tunnel pressures are measured using piezoresistive pressure transducers. Measurements of the pressures on the model are made by an automatic pressure-scanning system. Data are obtained and recorded with an electronic data-acquisition system.

Experimental Methods

The surface pressures measured on the model are reduced to standard pressure coefficients and numerically integrated to obtain section normal and chord-force coefficients, as well as the section pitching-moment coefficient about the quarter-chord point. Section profile-drag coefficients are computed from the wake total and static pressures using standard procedures [17]. Low-speed wind-tunnel boundary corrections are applied to the data [18]. A total-pressure-tube displacement correction, although quite small, is also applied to the wake-survey probe [17].

As is clear from the applying the procedures prescribed in [19], the uncertainty of a measured force or moment coefficient depends on the operating conditions and generally increases with increasing angles of attack. In the higher-lift regions, for which the uncertainty is the greatest, the measured lift coefficients have an uncertainty of $\Delta c_l = \pm 0.005$. The uncertainty of drag coefficients measured in the low-drag range is $\Delta c_d = \pm 0.00005$, and as the angle of attack

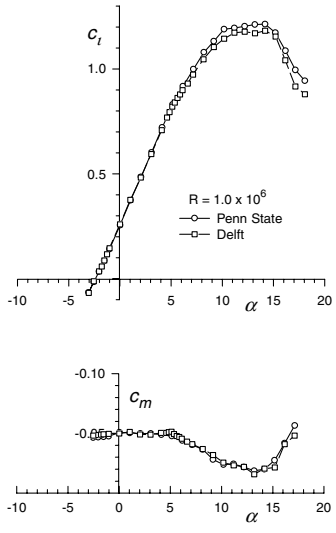

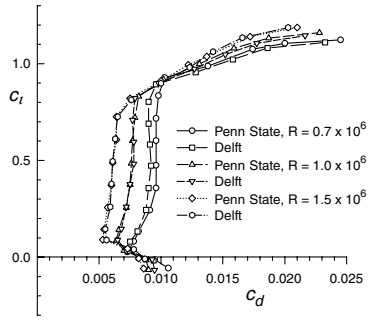

Fig. 2 Comparison of aerodynamic characteristics of the S805 airfoil measured in the low-speed wind tunnels at Pennsylvania State University and the Delft University of Technology.

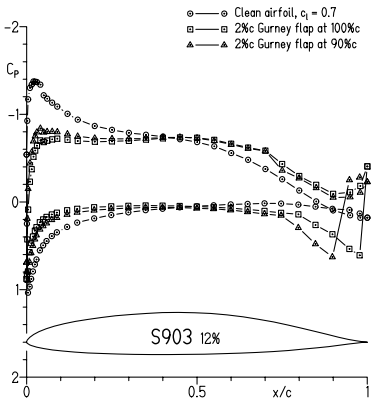

Fig. 3 Pressure distributions at a $c_l = 0.7$ with and without Gurney flaps.

approaches stall, this increases to $\Delta c_d = \pm 0.00015$. The pitching-moment coefficients have an uncertainty of $\Delta c_m = \pm 0.002$.

In addition to making the quantitative measurements indicated, flow-visualization studies were performed using fluorescent oil [20]. These methods were used not only to determine transition locations and regions of separated flow as they depend on angle of attack, but also to verify the two-dimensionality of the tests. As is typically the case in this facility, it was found that the flow over the model was two-dimensional up to and slightly beyond the angle of attack at which the maximum lift coefficient occurs.

Experimental Results

Pressure distributions of the baseline airfoil and those for the airfoil with a $0.02c$-high Gurney flap mounted at the 0.90 and $1.0c$ locations of the lower surface are shown in Figs. 3 and 4. The effects of the different chordwise locations at a constant lift coefficient of 0.7 are compared in Fig. 3, and pressure distributions at the maximum lift coefficients are shown in Fig. 4. The maximum lift coefficients are 1.15, 1.35, and 1.5 for the baseline airfoil and for the cases having the Gurney flap located at 0.90 and $1.0c$, respectively.

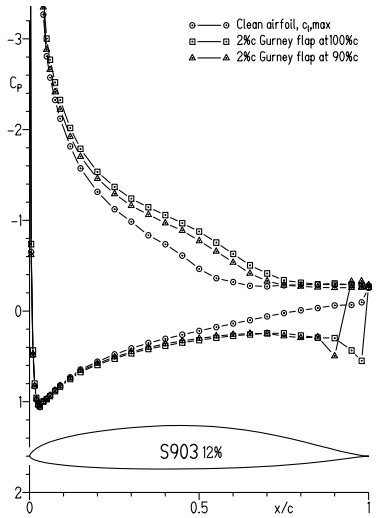

Fig. 4 Pressure distributions at a $c_{l\max}$ with and without Gurney flaps.

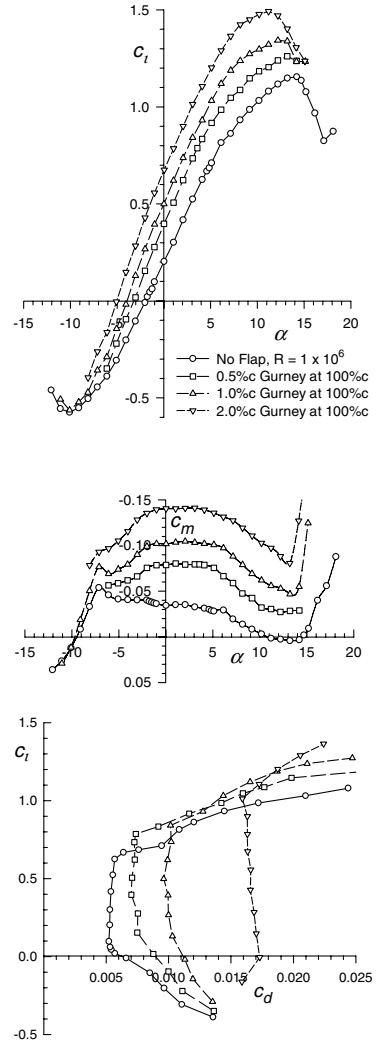

Fig. 5 Aerodynamic characteristics with varying Gurney flap height.

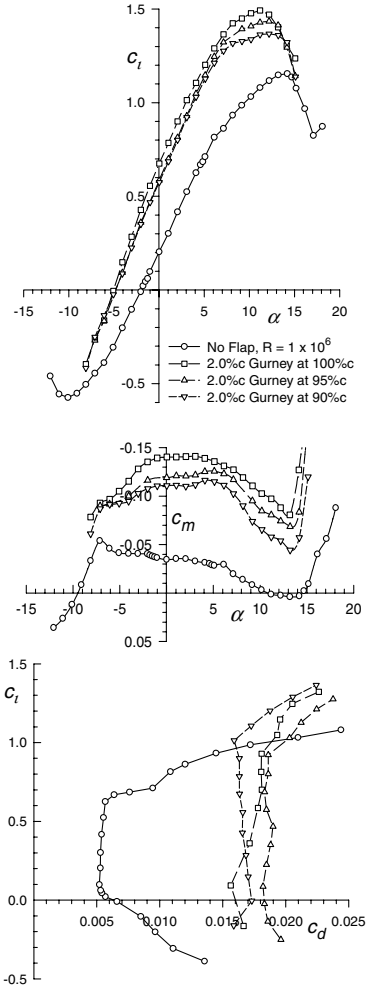

Fig. 6 Aerodynamic characteristics with varying Gurney flap chordwise location.

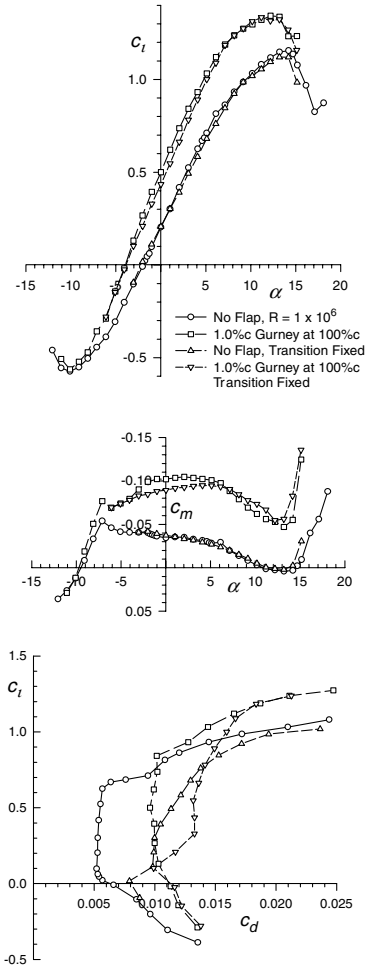

Fig. 7 Aerodynamic characteristics with natural transition and transition fixed at .02*c* on the upper surface and .05*c* on the lower.

In Fig. 3, it can be seen that the Gurney flap significantly increases the pressures on the lower surface of the airfoil just upstream of the flap. Downstream of the flap, a strong favorable pressure gradient leads to a trailing-edge pressure that is lower than that of the baseline airfoil. On the upper surface, the lowering of the trailing-edge pressures with the Gurney flaps reduces the leading-edge suction peak and postpones the start of the pressure recovery by almost 0.20*c*. The pressure recoveries occur with lower pressures than in the baseline case. This causes a relaxing of the adverse pressure gradient on the upper surfaces such that both Gurney flap configurations have longer runs of laminar flow than the baseline, followed by a small laminar separation bubble that forms at about 0.60 to 0.70*c*.

As can be observed in Fig. 4, the maximum lift-coefficient gains with the Gurney flap are due in large part to an increase in the lower-surface pressure upstream of the flap location. At the higher angles of attack, the thinning of the boundary layer of the lower surface results in an increasingly upstream spreading of the Gurney flap influence. Further lift gains are due to the lowering of the pressure levels of the recovery region on the upper surface. In these cases, the separation point moves aft from roughly 0.10 to 0.15*c* as the Gurney flap is moved from 0.90*c* to the trailing edge. At these angles of attack, the trailing-edge pressures of all three configurations are approximately equal. The difference in maximum lift between the two Gurney flap configurations is primarily explained by the earlier pressure drop on the lower surface, which occurs when the Gurney flap is positioned more forward, and the subsequent loss of lift production from the flap location up to the trailing edge.

The influence of the Gurney flap height on the aerodynamic characteristics is shown in Fig. 5. Compared with the baseline airfoil, the Gurney flap that is 0.02*c* high and located at the trailing edge achieves a 29% increase in the maximum lift coefficient. The smaller flaps have gains in the maximum lift coefficient that are roughly proportional to their size. As the boundary layer thins on the lower surface with increasing angles of attack, the Gurney flap on that surface becomes more effective and the lift generated increases. Likewise, the impact of a Gurney flap diminishes as the angle of attack decreases, resulting in a converging of the lift curves toward the negative maximum lift coefficient. As a consequence of the Gurney flap effectiveness depending on the angle of attack, the lift-curve slope increases with the height of the Gurney flap. The moment-coefficient curves behave similarly, in that they merge with increasingly negative angle of attacks. At angles of attack for which the Gurney flap is effective, the increased aft loading due to the flap results in pitching-moment coefficients that are more nose-down than those of the baseline airfoil. The changes in pitching-moment coefficients are again roughly proportional to the Gurney flap height, as is (within the low-drag angle-of-attack region) the increase in the minimum drag coefficient.

Some schemes involving deployable Gurney flaps (MiTEs) require that they be located far enough forward of the trailing edge to be completely buried within the airfoil when not deployed. As is demonstrated by the results presented in Fig. 6, the aerodynamic gains achieved with Gurney flaps are only moderately reduced by upstream mounting locations. The maximum achievable lift coefficient is reduced by approximately 10% as the flap location is moved from the trailing edge to 0.90*c*. The changes in the moment coefficient are of similar magnitudes, whereas the drag characteristics are more influenced by the height of the Gurney flap than by its chordwise location.

As noted, the S903 airfoil was designed for significant amounts of laminar flow. To explore how Gurney flaps and MiTEs would affect

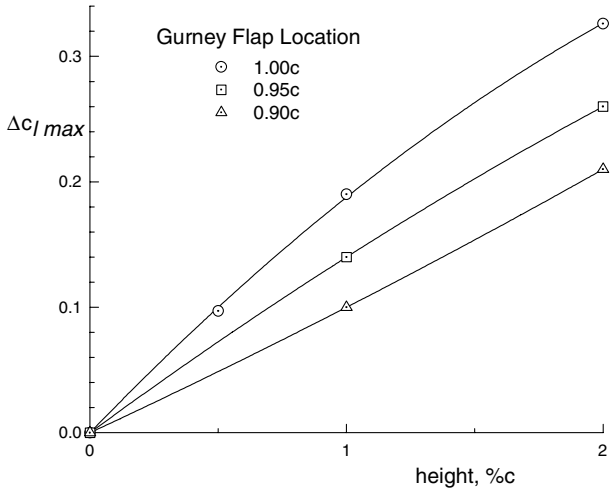

Fig. 8 Change in maximum lift coefficient with varying Gurney flap heights and chordwise locations.

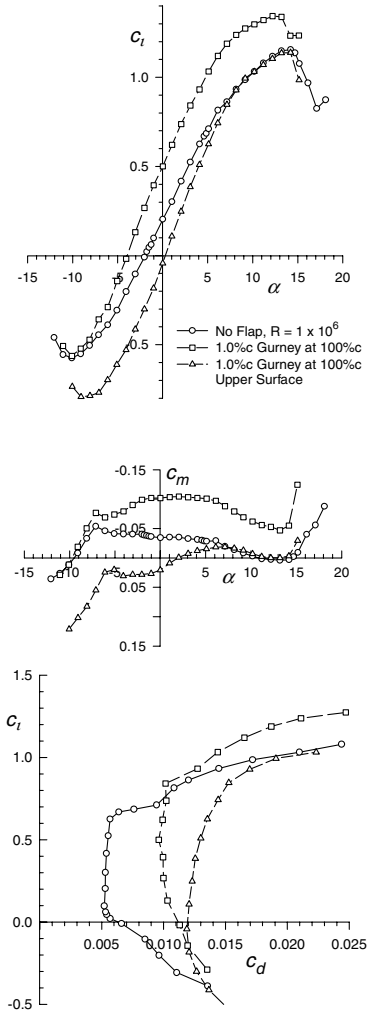

Fig. 9 Comparison of the aerodynamic characteristics with a .01*c*-high Gurney flap located at the trailing edge on the upper and lower surfaces.

the aerodynamics of traditional airfoils not designed for extended runs of laminar flow, measurements were made on the S903 with transition fixed at $0.02c$ on the upper and $0.05c$ on the lower surfaces. Because the primary interest is on the aerodynamic behavior near the maximum lift coefficient, the turbulator grit was sized to the critical roughness height for angles of attack approaching stall [21]. Thus, at lower angles of attack, the grit size is too small to force transition. This is demonstrated in Fig. 7 by the converging of the free- and fixed-transition drag curves at low angles of attack. As also observed in this figure, although the drag increases as expected with fixed transition, the lift and moment curves are essentially unaffected. With fixed transition, the drag increase due to the Gurney flap is not nearly as large as it is with free transition, especially in the case of the baseline airfoil that has significant amounts of laminar flow. The fixed-transition cases are more likely to be representative of what is expected for an airfoil not designed for extended laminar flow.

Based on results such as the preceding, the effects of Gurney flap height and location are summarized in Fig. 8. These plots should prove useful in the preliminary sizing of Gurney flaps for various applications.

Concerns about whether or not MiTEs can be used as control devices with up and down deployment are addressed by the data presented in Fig. 9, in which the effects of a $0.01c$-high Gurney flap on the upper surface with those of one on the lower surface are compared. The Gurney flap on the upper surface becomes effective as the angle of attack decreases and the boundary layer on the upper surface thins. At higher angles of attack, its aerodynamic characteristics merge with those of the baseline airfoil. For a lower-surface Gurney flap, the opposite is true. It becomes more effective with increasing angles of attack, whereas at lower angles of attack, its aerodynamic characteristics merge with those of the baseline. Although at midrange angles of attack, MiTEs still have a significant effect on lift and moment, an upward-deploying MiTE will have no control effectiveness on a surface approaching a positive angle-of-attack stall, and a downward-deploying MiTE will have no effect on a surface approaching a negative angle-of-attack stall.

Conclusions

The changes in airfoil aerodynamics due to Gurney flaps of varying sizes and locations at and near the trailing edge were explored experimentally using the Pennsylvania State University low-speed low-turbulence wind tunnel. The results obtained using surface-pressure integration are in general agreement with those obtained by other researchers using force balances. The high-quality drag data and surface-pressure distributions presented here help to understand and predict the aerodynamic behavior of Gurney flaps. In addition, the experimental results provide valuable data for the validation of computational methods.

The lift gains with Gurney flaps attached to the lower surface are due in large part to an increase in the lower-surface pressures upstream of the flap location. At the higher angles of attack, the influence of the Gurney flap spreads increasingly forward. Further lift gains are due to a lessening of the adverse recovery gradients on the upper surface, thus moving the point at which the flow separates aft. In addition, for the case of an extended laminar-flow airfoil, the value of the minimum drag varies nearly linearly with the Gurney flap height, whereas the flap location has less influence on the drag. For the fixed-transition cases, the relative increase in drag due to the Gurney flap is less severe. Finally, as a consequence of the aft loading that is a consequence of the Gurney flap effect on the pressure distribution, a Gurney flap increases the amount of nose-down pitching moment.

References

[1] Liebeck, R. H., "Design of Subsonic Airfoils for High Lift," *Journal of Aircraft*, Vol. 15, No. 9, September 1978, pp. 547–561. doi:10.2514/3.58406

[2] Myose, R., Papadakis, M., and Heron, I., "Gurney Flap Experiments on Airfoils, Wings, and Reflection Plane Model," *Journal of Aircraft*, Vol. 35, No. 2, Mar.–Apr. 1998, pp. 206–214.

[3] Jeffrey, D. R. M., Zhang, X., and Hurst, D. W., "Aerodynamics of Gurney Flaps on a Single-Element High-Lift Wing," *Journal of Aircraft*, Vol. 37, No. 2, Mar.–Apr. 2000, pp. 295–301.

[4] Kentfield, J. A. C., "The Potential of Gurney Flaps for Improving the Aerodynamic Performance of Helicopter Rotors," AIAA International Powered Lift Conference, AIAA Paper 93-4883, 1993, pp. 283–292.

[5] Kroo, I. M., "Aerodynamic Concepts for Future Aircraft," AIAA Applied Aerodynamics Conference, AIAA Paper No. 99-3524, 1999.
[6] Bieniawski, S., and Kroo, I. M., "Flutter Suppression Using Micro-Trailing Edge Effectors," AIAA Paper 2003-1941, 2003.
[7] Maughmer, M., Lesieutre, G., and Kinzel, M. P., "Miniature Trailing-Edge Effectors for Rotorcraft Performance Enhancement," *Journal of the American Helicopter Society*, Vol. 52, No. 2, Apr. 2007, pp. 146–158.
[8] Yen-Nakafuji, D. T., van Dam, C. P., Smith, R. L., and Collins, S. D., "Active Load Control for Airfoils Using Microtabs," *Journal of Solar Energy Engineering*, Vol. 123, No. 4, Nov. 2001, pp. 282–289. doi:10.1115/1.1410110
[9] Brophy, C. M., "Turbulence Management and Flow Qualification of the Pennsylvania State University Low Turbulence, Low Speed, Closed Circuit Wind Tunnel," M.S. Thesis, Dept. of Aerospace Engineering, Pennsylvania State Univ., University Park, PA, 1993.
[10] McGhee, R. J., Beasley, W. D., and Foster, J. M., "Recent Modifications and Calibration of the Langley Low-Turbulence Pressure Tunnel," NASA TP-2328, 1984.
[11] van Ingen, J. L., Boermans, L. M. M., and Blom, J. J. H., "Low-Speed Airfoil Section Research at Delft University of Technology," International Council of the Aeronautical Sciences Paper 80-10.1, Oct. 1980.
[12] McGhee, R. J., Walker, B. S., and Millard, B. F., "Experimental Results for the Eppler 387 Airfoil at Low Reynolds Numbers in the Langley Low-Turbulence Pressure Tunnel," NASA TM 4062, Oct. 1988.
[13] Somers, D. M., and Maughmer, M. D., " Experimental Results for the E 387 Airfoil at Low Reynolds Numbers in the Pennsylvania State University Low-Speed, Low-Turbulence Wind Tunnel," U.S. Army Research, Development and Engineering Command, TR 07-D-32, Moffett Field, CA, May 2007.
[14] Medina, R., "Validation of the Pennsylvania State University Low-Speed, Low-Turbulence Wind Tunnel Using Measurements of the S805 Airfoil," M.S. Thesis, Dept. of Aerospace Engineering, Pennsylvania State Univ., University Park, PA, 1994.
[15] Somers, D. M., "Design and Experimental Results for the S805 Airfoil," National Renewable Energy Lab. Rept. SR-440-6917, Golden, CO, Oct. 1988.
[16] Somers, D. M., "Effects of Airfoil Thickness and Maximum Lift Coefficient on Roughness Sensitivity," National Renewable Energy Lab. Rept. SR-500-36336, Golden, CO, Jan. 2005.
[17] Prankhurst, R. C., and Holder, D. W., *Wind-Tunnel Technique*, Sir Isaac Pitman & Sons, London, 1965.
[18] Allen, H. J., and Vincenti, W. G., "Wall Interference in a Two-Dimensional-Flow Wind Tunnel, with Consideration of the Effect of Compressibility," NACA Rept. 782, 1944.
[19] Anon., *Assessment of Experimental Uncertainty with Application to Wind Tunnel Testing*, AIAA Rept. S-071A-1999, Rev. A, Reston, VA, 1999.
[20] Loving, D. L., and Katzoff, S., "The Fluorescent-Oil Film Method and Other Techniques for Boundary-Layer Flow Visualization," NASA Rept. 3-17-59L, 1959.
[21] Braslow, A. L., and Knox, E. C., "Simplified Method for Determination of Critical Height of Distributed Roughness Particles for Boundary-Layer Transition at Mach Numbers From 0 to 5," NACA TN 4363, 1958.